

5 Numerical Modeling

Modeling has been a useful tool for engineering design and analysis. The definition of modeling may vary depending on the application, but the basic concept remains the same: the process of solving physical problems by appropriate simplification of reality. In engineering, modeling is divided into two major parts: physical/empirical modeling and theoretical/analytical modeling. Laboratory and in situ model tests are examples of physical modeling, from which engineers and scientists obtain useful information to develop empirical or semi-empirical algorithms for tangible application. Theoretical modeling usually consists of four steps. The first step is construction of a mathematical model for corresponding physical problems with appropriate assumptions. This model may take the form of differential or algebraic equations. In most engineering cases, these mathematical models cannot be solved analytically, requiring a numerical solution. The second step is development of an appropriate numerical model or approximation to the mathematical model. The numerical model usually needs to be carefully calibrated and validated against pre-existing data and analytical results. Error analysis of the numerical model is also required in this step. The third step of theoretical modeling is actual implementation of the numerical model to obtain solutions. The fourth step is interpretation of the numerical results in graphics, charts, tables, or other convenient forms, to support engineering design and operation.

With increase in computational technology, innumerable numerical models and software have been developed for various engineering practices. Numerical modeling has been used extensively in industries for both forward problems and inverse problems. Forward problems include simulation of space shuttle flight, ground water flow, material strength, earthquakes, and molecular and medication formulae studies. Inverse problems consist of non-destructive evaluation (NDE), tomography, source location, image processing, and structure deformation during loading tests. Although

numerical models enable engineers to solve problems, the potential for abuse and misinformation persists. Colorful impressive graphic presentation of a sophisticated software package does not necessarily provide accurate numerical results. Fundamental scientific studies and thorough understanding of the physical phenomena provide a reliable and solid guideline for engineering modeling. In this project, the focus is on the thermo effects of drilled shafts after the placement of concrete, and performance under various loading conditions. The numerical models developed in this project are based on well-developed theories and constitutive laws in chemical and civil engineering, as well as numerical methods widely accepted in engineering. The numerical results are also carefully analyzed against existing laboratory test data.

5.1 Establishment of Numerical Model

Modeling is fundamentally the core of engineering. A model is an appropriate simplification of reality. The skill in modeling is to spot the appropriate level of simplification, distinguish important features from those that are unimportant in a particular application, and use engineering judgment. There is a long history of empirical modeling in civil engineering. Due to difficulties in obtaining accurate material properties of in situ earth materials and construction materials, most civil engineering is based on experience--although many techniques are semi-empirical rather than purely empirical. For this reason, the development of more rigorous modeling tools has lagged behind the demands of industry. In this project, advancements in computational techniques, civil engineering, and material science are incorporated into a theoretical/mathematical numerical model based on the analysis of physical phenomena and constitutive laws for the application of drilled shafts in roadway/highway engineering.

5.2 Theoretical Models

The description of most engineering problems involves identifying key variables and defining how these variables interact. The study of theoretical modeling involves two important steps. In the first step, all the variables that affect the phenomena are identified, reasonable assumptions and approximations are made, and the interdependence of these variables is studied. The relevant physical laws and principles are invoked, and the problem is formulated mathematically. In the second step, the problem is solved using an appropriate approach (in this project, an appropriate numerical approach) and results are interpreted.

The fundamental principles and constitutive laws of material behavior have been thoroughly investigated for engineering purposes. This makes it possible to predict the course of an event before it actually occurs, or to study various aspects of an event mathematically without actually running expensive and time-consuming experiments. Very accurate results to meaningful practical problems can be obtained with relatively little effort by using suitable and realistic mathematical/numerical models. However, the preparation of such models requires an adequate knowledge of the natural phenomena and relevant laws, as well as sound judgment.

Theoretical modeling leads to an analytical solution of the problem. For this reason, engineering problems are often described by differential equations. An engineer often has to choose between a more accurate but complex model, and a simple but relatively less accurate and over-generalized model. Available computational technology and techniques provide engineers the option of exploring complex numerical models. A numerical solution usually implies the replacement of a continuous description of a problem by one in which the solution is only obtained at a finite number of points in space and time. In this project, the quality of the numerical

approach is verified by applying the numerical model to a situation for which an exact solution is known.

However, mathematical/numerical modeling does not eliminate the indispensable experimental approach to physical modeling. The experimental approach provides observations of actual physical phenomena. Physical modeling is fundamental in the development of civil engineering. Many theoretical and empirical models are based on the interpretation of experimental results. Physical modeling validates the theoretical and empirical hypotheses. However, this approach is expensive, time-consuming, and not always practical in engineering.

The theoretical models and technical approaches employed in this project to model the drilled shaft in highway engineering are: a) thermal modeling; b) engineering mechanics; c) numerical model of discrete element method (DEM) and d) validations of numerical models.

5.3 Thermal Modeling

It is well known that the thermal behavior, temperature distribution, and residual stresses/strains in the shaft during concrete placement significantly affect the performance and strength of the support. In this section, heat transfer and the resulting temperature gradient will be discussed. A chemical model and heat transfer model were implemented together with a mechanics constitutive model to simulate conditions of the concrete shaft while curing.

During the concrete curing (hydration) process, heat generates inside of the concrete. This heat transfers from regions of higher temperature to regions of lower temperature, such as the surrounding environment. The non-uniform temperature gradient causes variations in shrinkage strains and generates cracks in the shaft. Common guidelines specify a 20° C (35° F) temperature gradient rule, restricting the

maximum temperature difference in the concrete. The 20° C rule may not truly reflect all situations, as the heat of hydration, thermal conductivity, tensile strength, modulus, and density of concrete changes as a function of time. Contractors often find difficulty maintaining high concrete strength by using a higher percentage of cement paste, which generates more heat, and still satisfy the temperature gradient rule. The heat transfer model employed in this project tries to combine curing chemistry, aging, thermal behavior, and mechanical strength of concrete to provide a better understanding of the concrete curing process so that appropriate engineering limits may be developed for temperature and quality control.

The rate of heat generation during concrete curing varies with temperature and time. The temperature inside a shaft varies with time, as well as position. This variation is expressed as:

$$T(\mathbf{x}, t), \tag{5.1}$$

where

\mathbf{x} is the position vector

t is time

The conductivity of concrete during curing varies with time and position, expressed as:

$$k(\mathbf{x}, t) \tag{5.2}$$

This case is a typical nonlinear unsteady 3D heat conduction problem. Unfortunately, an analytical solution of the problem does not exist, except for overly simplified conditions. Numerical modeling can provide an efficient technical approach for this problem. In order to accurately model the thermal behavior during the curing process, a modified 3D explicit finite difference model is used as the numerical

method in this study. Basic principles of the numerical solution and algorithm are presented in this section. Note that heat transfer by convection is considered, but heat transfer by radiation is not considered in this study.

The 3-dimensional heat conduction equation is expressed as:

$$\nabla(k_i \nabla T) + \dot{g} = \rho c \dot{T} \quad (5.3a)$$

Or, in the rectangular coordinate system as:

$$\frac{\partial}{\partial x} k_x(\mathbf{x}, t) \frac{\partial T(\mathbf{x}, t)}{\partial x} + \frac{\partial}{\partial y} k_y(\mathbf{x}, t) \frac{\partial T(\mathbf{x}, t)}{\partial y} + \frac{\partial}{\partial z} k_z(\mathbf{x}, t) \frac{\partial T(\mathbf{x}, t)}{\partial z} + \dot{g}(\mathbf{x}, t) = \rho c \frac{\partial T(\mathbf{x}, t)}{\partial t} \quad (5.3b)$$

Where

$T(\mathbf{x}, t)$ is the temperature distribution function with element control volume as $dx dy dz$

$k_i(\mathbf{x}, t)$ is the thermal conductivity in corresponding directions, respectively

$\dot{g}(\mathbf{x}, t)$ is the rate of energy generation in the control volume

ρ is density of the material

c is specific heat (The heat capacity per unit of mass of the object)

\mathbf{x} is position vector variable, explicitly expressed as x, y and z in rectangular coordinates

t is time

The solution of equation (5.3) gives the temperature distribution in the material at different times. The temperatures obtained are used as input to the concrete curing chemistry model and engineering mechanics model to determine concrete tension/compression strength and thermal stresses/strains. Crack formation occurs

when the tension stress is larger than the tension strength at a certain position. Cracks are simulated by breaking the connection between the material points. Micro-cracks develop and propagate inside the concrete as more connections are broken. These defects are taken into account for the concrete shaft loading and performance analysis. The model in this project is developed to represent history dependent material behavior.

Equation (5.3) is a non-linear unsteady heat conduction equation. Various numerical methods have been developed for the finite solution. One of the most popular is the finite difference method, which discretizes the domain into a finite mesh or grid. Equation (5.3) is solved on the mesh nodes together with boundary and initial conditions. The accuracy and efficiency of the solution depend on the discretization method, mesh size, and numerical integration algorithm. Generally, the mesh size is cubic in rectangular coordinates, or curved cubic in cylindrical or spherical coordinates. In this project, a modified finite difference solution was developed with mesh nodes connected in a tetrahedral packing form that matches the mechanics numerical analysis algorithm. Figure 5.1 shows a portion of a 2D and 3D thermal resistance network mesh and nodes connection for heat conducting calculations.

The solution algorithm is based on the well known thermal resistance concept in thermal dynamics. Heat conduction is analogous to the relation for electric current flow as shown in Figure 5.1. According to Fourier's law of heat conduction, the rate of heat conduction through a plane layer is proportional to the temperature difference across the layer and the heat transfer area, but is inversely proportional to the thickness of the layer. Assume that at given time the distance between two adjacent nodes is Δx , the temperature difference is ΔT , which equals to the temperature at

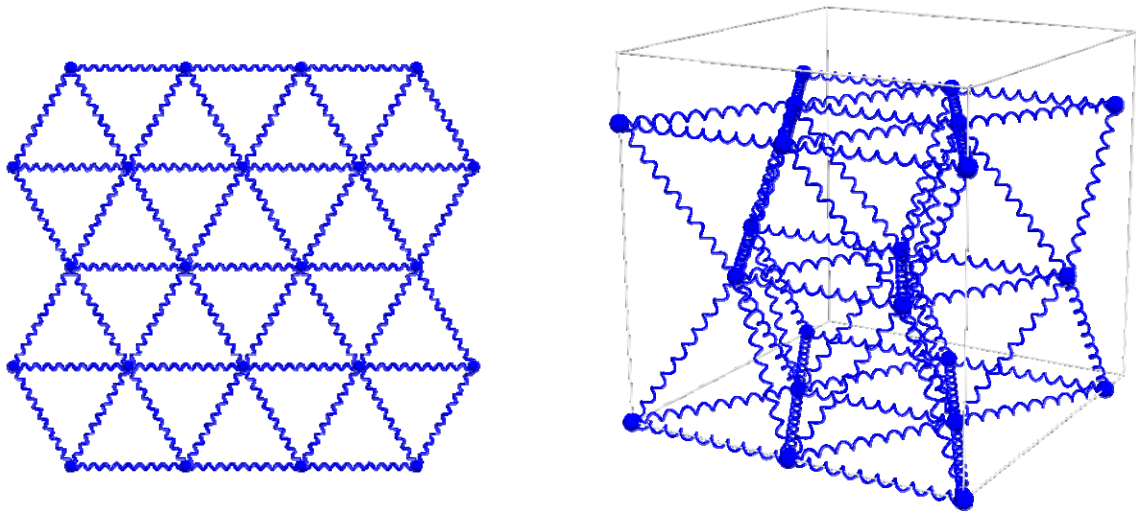


Figure 5.1 2D and 3D Thermal Network Mesh for Heat Conducting Calculations

node 1 (T_1) minus the temperature at node 2 (T_2). Defining the heat conduction area between two nodes as A gives:

$$\dot{q} = kA \frac{\Delta T}{\Delta x} = kA \frac{T_1 - T_2}{\Delta x} \quad (5.4)$$

where

k is thermal conductivity, a function of time and location.

By using the thermal resistance concept, equation (5.4) can be rewritten as:

$$\dot{q} = \frac{\Delta T}{R_{i-n}} = \frac{T_1 - T_2}{R_{i-n}} \quad (5.5)$$

where

R_{i-n} is thermal conduction resistance between node i and node n :

$$R_{i-n} = \frac{\Delta x}{kA} \quad (5.6)$$

Assuming that the conduction area A is constant between two nodes, and the mesh grid size is generated equally so that Δx is constant, R_{i-n} is only a function of k . In thermal modeling R_{i-n} is the variable vector of time and position. R_{i-n} is appropriately defined based on the concrete curing chemistry model. For 3D tetrahedral packing connections, each node is connected to twelve other neighbor nodes to form a thermal resistance network covering the model domain.

Assuming the initial temperature of concrete at placement is T_0 , and assuming the heat generated by a unit concrete mass while curing is q (a function of concrete hydration rate), the temperature raised by unit mass due to the generated heat energy is:

$$\Delta T = \frac{q}{c} \quad (5.7)$$

where

ΔT is the temperature change per unit concrete mass due to the heat generated in hydration

c is the specific of heat of concrete

The specific heat is defined as the energy required to raise the temperature of a unit mass of a substance by one degree. Specific heat is a material property and is physically measured at constant volume (c_v) or constant pressure (c_p). Generally it is a function of temperature, though the change is small. Since concrete changes from a “fluid” state to a solid state while curing, the specific heat also changes correspondingly. For this reason, the specific heat is also a function of hydration. In

this study, the change of specific heat is assumed to be linear to the non-linear hydration rate.

After the temperatures at each calculation mesh node are known, equation (5.5) is used to calculate the heat transfer rate between nodes. The heat energy at each node is updated correspondingly, based on the heat transfer rate changes. The new heat energy is then used to update the temperature of each node. Since the numerical modeling is based on a dynamic algorithm, and the temperature of boundary nodes are constrained by boundary conditions, the boundary conditions are correspondingly satisfied in the simulation.

5.4 Engineering Mechanics

In this section, the basics of the engineering mechanics principles involved in the modeling and analysis of this project are briefly presented. Since design philosophies, failure criteria, load capacity evaluation methods, and building codes for drilled shafts have been well defined in highway/roadway and civil engineering in AASHTO publications and other engineering resources, these topics will not be repeated. The focus is on the mechanical properties of concrete and soil, their relation to stress wave propagation in these materials, and the effect of thermal cracking and other defects to the performance of drilled shafts.

When an impact load is applied to a body, the deformation of the body due to the load will gradually spread throughout the body via stress waves. The nature of propagation of stress waves in an elastic medium is extremely important in geotechnical and geophysical engineering. Even though the materials encountered in geotechnical and geophysical engineering can hardly be called “elastic”, the theory developed for an elastic medium is very useful and satisfactory in signal processing and inverse problem analysis. It is also widely used to determine material properties

such as elastic modulus and shear modulus, and other design parameters of dynamic load-resistant structures.

From continuum mechanics theory, the equation of motion in an elastic medium can be written as:

$$\frac{\partial \sigma_{ij}}{\partial x_j} = \rho \frac{\partial^2 u_i}{\partial t^2} \quad (5.8)$$

where

σ_{ij} is the stress tensor

u_i is the displacement vector

ρ is the density of the material

By substituting the elastic stress-strain relationship into the equation of motion and re-arranging the equations, the elastic compression stress wave equation becomes:

$$\frac{\partial^2 p}{\partial t^2} = c_p^2 \nabla^2 p \quad (5.9)$$

where

p is the pressure

∇^2 is the Laplacian

c_p is the P-wave velocity

The elastic shear stress wave equation can be expressed as:

$$\frac{\partial^2 \omega_i}{\partial t^2} = c_s^2 \nabla^2 \omega_i \quad (5.10)$$

where

ω_i is the rotation vector

c_s is the S-wave velocity

From the above equations, the relationship of P-wave and S-wave velocity and elastic material properties are defined as:

$$c_p = \sqrt{\frac{\lambda + 2G}{\rho}} = \sqrt{\frac{E(1 - \mu)}{\rho(1 + \mu)(1 - 2\mu)}} \quad (5.11)$$

$$c_s = \sqrt{\frac{G}{\rho}} = \sqrt{\frac{E}{2(1 + \mu)\rho}} \quad (5.12)$$

where

E is the elastic modulus

G is the elastic shear modulus

λ is the Lamé constant

μ is the Poisson's ratio

Note that the material constants during concrete curing are a function of time and temperature. The actual values applied for the calculations in this project are based on the concrete curing chemistry modeling results.

The visco-elastic model is considered a better approach to wave propagation in geo-materials since the amplitude of the source wave attenuates with distance. The corresponding visco-elastic wave equation can be derived based on the equation of motion with a damping force:

$$\frac{\partial \sigma_{ij}}{\partial x_j} = \rho \frac{\partial^2 u_i}{\partial t^2} + c \frac{\partial u_i}{\partial t} \quad (5.13)$$

where

c is damping coefficient of the medium.

The solutions of equations (5.9) and (5.10) describe wave propagation in an elastic medium. In geophysics, the finite difference method (FD) is the most common numerical method chosen for the solution. Various numerical schemes can be considered for the finite difference solution. For a 3D problem, various schemes include cubic rectilinear, octahedral, interpolated rectilinear, or tetrahedral, depending on the specific problem and desired accuracy. In this project, a non-linear visco-elastic model is used for the wave propagation calculations.

Thermal stress calculations during concrete curing are based on chemistry modeling. The stress depends on curing temperature, concrete strength and strain at different curing stages. The relationship between the rate of change of the temperature and strain with heat conduction is given by:

$$\frac{\partial}{\partial x_i} \left(k_{ij} \frac{\partial T}{\partial x_j} \right) = \rho C_v \frac{\partial T}{\partial t} + T \beta_{ij} \frac{\partial \varepsilon_{ij}}{\partial t} \quad (5.14)$$

where

β_{ij} is a material constant proportional to the temperature change

k_{ij} is the thermal conductivity matrix

C_v is the specific heat per unit mass measured in the state of constant strain

ρ is the density of the material

ε_{ij} is the strain tensor

T is the temperature

Again the material constants of concrete during curing depend on the temperature and the time. The constant values are obtained from concrete curing chemistry modeling and analysis.

To complete the specification of the mechanical properties of a material, additional constitutive equations are developed for the concrete curing process. The mechanical constitutive equation of a curing concrete specifies the dependence of stress on kinematics variables such as the rate of deformation tensor, temperature and other thermodynamics, electrostatics, and chemical variables. Since this study focuses on engineering application, more effort is concentrated on the simplification of currently available theoretical equations, and calibration of numerical models to meet the accuracy of engineering practice. Detailed descriptions of the technical approaches for concrete and soil is presented in the following sections.

5.5 Discrete Element Method (DEM) Background

Numerical modeling of the discrete element method and its application is presented. As discussed earlier, most mathematical equations established in theoretical modeling cannot be solved analytically, requiring a numerical solution. The development and selection of an appropriate numerical model is a key step for the successful application. Many numerical methods have been developed to solve different engineering problems, such as the Finite Element Method (FE), Finite Difference Method (FD), Boundary Value Problem (BV), Discrete Element Method (DEM), Material Point Method (MPM), etc. No single numerical method has been shown to be sufficient for all engineering problems. Each method has advantages and limitations for particular problems. The more physical phenomena are understood, the better numerical techniques can be developed and applied. In this project, the discrete element method (DEM) is employed based on the following considerations:

- **Simplicity:** the algorithm is simple to implement.
- **Efficiency:** the data structure of DEM is based on a mesh free principle, resulting in efficient computation and memory usage. The numerical model can be run on normal PC environments at high resolution.
- **Flexibility:** the model is originally designed for dynamics problems, such as wave propagation, contact/impact, and vibration problems. It can be easily modified to solve other problems, such as statics problems with dynamic relaxation, heat transfer problems with thermal resistance, seepage problems with friction losses, etc. The model simplifies generation of different geometrical shapes and boundary conditions.
- **Extensibility:** the model can be easily extended for geotechnical engineering applications such as slope stability, ground-foundation interactions, rock falls, tunneling/mining operations, avalanche study, as well as granular flow problems in chemical engineering and agricultural industries.

DEM, as well as any other numerical method, has limitations in engineering applications. Since the modeling domain of DEM is discretized into distinct particles which contact each other at their contact faces, the contact constitutive equations between particles determine the global mechanical responses of the whole particle assembly. The simplest contact constitutive model is represented by spring-dashpot model for a normal contact, and Coulomb friction model for shear force, as shown in Figure 5.2. Although these constitutive models do not necessarily have to be linear and elastic, the model currently uses linear and elastic deformation unless the particles are totally detached. For the same discretization scheme of DEM, each individual particle is considered a “rigid” body. There is no deformation for individual particles. If such deformation is desired, a combined approach of DEM with other numerical methods such as FE or BV is usually used. The contact

constitutive model in this project is based on a non-linear contact mechanics model between two spheres.

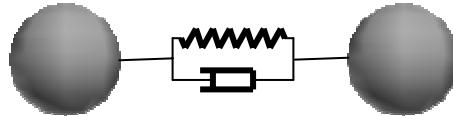


Figure 5.2 Visco-Elastic Contact Model for DEM

5.5.1 Discrete Element Method Definition

The discrete element method (DEM) is a numerical technique designed to solve problems in applied mechanics that exhibit gross discontinuous material and geometrical behavior. DEM is used to analyze multiple interacting rigid or deformable bodies undergoing large dynamic or pseudo static, absolute or relative motion, governed by complex constitutive behavior.

DEM essentially is based on the numerical solution of the equation of motion and the principle of dynamic relaxation. Kinematics equations are established for each discrete body. The velocities, accelerations, and positions of the bodies are updated by calculating the contact forces between them. Depending on different physical problems, DEM programs should at least include the following three aspects:

- Representation of contact, which attempts to establish a correct contact constitutive model between discrete bodies.
- Representation of the properties of materials, which defines the particles or blocks to be rigid or deformable.

- Contact detection and revision of contacts, which attempts to establish certain data structures and algorithms to assess the contacts and the contact types, such as whether the vertex, edge or face of one polyhedron will touch a corresponding entity on a second polyhedron.

The following section discusses the discrete element method specifically related to this project, which discretizes the particles as 3D spheres that contact each other at their surfaces. Some general features of DEM are also included in this section.

5.5.2 Equation of Motion

Figure 5.3 shows two blocks **I** and **II** in contact. Their positions are defined by vectors \mathbf{R}_I and \mathbf{R}_2 . The blocks have masses m_1 and m_2 , linear velocity vectors \mathbf{v}_1 and \mathbf{v}_2 , and angular velocity vectors ω_1 and ω_2 . The equation of motion for element i at discretized time step n is:

$$\mathbf{M}_i \mathbf{a}_n^i + \mathbf{C}_i \mathbf{v}_n^i + \mathbf{P}_i(\mathbf{x}_n^i) = \mathbf{f}_n^i \quad (5.15)$$

where

\mathbf{x}_n^i , \mathbf{v}_n^i and \mathbf{a}_n^i are the position, velocity and acceleration vectors of the i th element at the n th time step,

$$\begin{aligned} (\mathbf{x}_n^i)^T &= [\mathbf{x}_n^i, \mathbf{y}_n^i, \mathbf{z}_n^i, \theta_n^i] \\ (\mathbf{v}_n^i)^T &= [\dot{\mathbf{x}}_n^i, \dot{\mathbf{y}}_n^i, \dot{\mathbf{z}}_n^i, \dot{\theta}_n^i] \\ (\mathbf{a}_n^i)^T &= [\ddot{\mathbf{x}}_n^i, \ddot{\mathbf{y}}_n^i, \ddot{\mathbf{z}}_n^i, \ddot{\theta}_n^i] \end{aligned} \quad (5.16)$$

where

\mathbf{M}_i and \mathbf{C}_i are the mass and damping matrices.

\mathbf{P}_i and \mathbf{f}_n^i are the resultant contact force and applied boundary force/body force, respectively.

The formula for contact force depends on the particular constitutive laws applied to the problems. A modified Hertz-Mindline contact law and visco-elastic contact law are discussed later in “Contact Mechanics”.

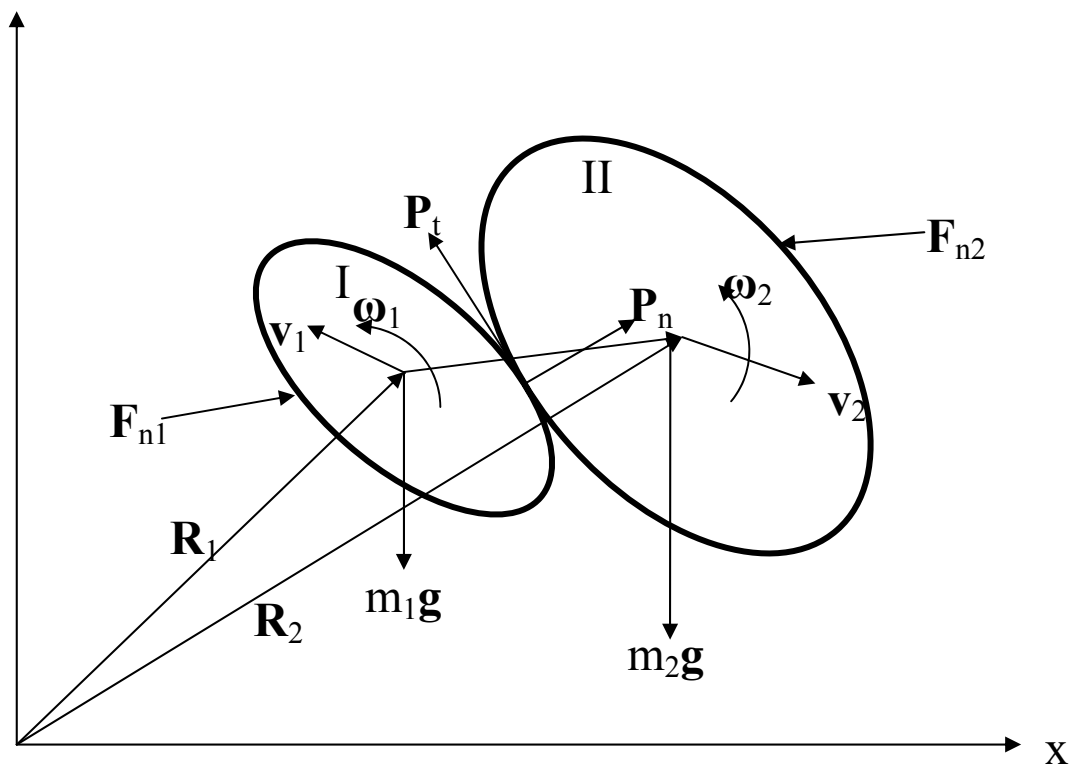


Figure 5.3 Blocks in Contact

Numerically solving equation (5.15) in the time domain gives accelerations, velocities, displacements and resultant forces. The stress/strain relationship inside of the discrete assembly is obtained by an averaging method. The *average stress tensor* of the volume V of the *representative of volume element* (RVE) can be obtained by:

$$\bar{\sigma}_{ij} = \frac{1}{V} \sum_{p=1}^N \sum_{c=1}^{m_p} \mathbf{x}_i^c \mathbf{F}_j^c \quad (5.17)$$

where

\mathbf{x}_i^c is position vector at contact point c

\mathbf{F}_j^c is contact force vector at contact point c

N is the particle number in RVE

m_p is the number of contact points for particle p

Similarly, the **average strain** of the RVE defined for infinite deformation can be written (by the Average Displacement Gradient Algorithm) as:

$$\bar{\varepsilon}_{ij} = \frac{1}{2} (\mathbf{F}_{ij} + \mathbf{F}_{ji}) \quad (5.18)$$

where

\mathbf{F}_{ij} is contact force

There are different numerical integration algorithms for solving equation (5.15). The explicit integration algorithm is among the most used schemes in current discrete element analysis. In this project, central different explicit expressions are used for the acceleration at time step interval h for velocity and displacement updates. The velocity update equation is:

$$\mathbf{v}_{n+1/2} = \frac{(M/h - C/2)}{(M/h + C/2)} \mathbf{v}_{n-1/2} + \frac{\mathbf{f}_n - \mathbf{P}}{(M/h + C/2)} \quad (5.19)$$

and the displacement update equation is:

$$\mathbf{x}_{x+1} = \mathbf{x}_n + h\mathbf{v}_{n+1/2} \quad (5.20)$$

Where the symbols are the same as in equation (5.15)

The explicit integration algorithm used in DEM analysis is quite simple and straightforward compared to implicit schemes. However, this algorithm is only conditionally stable. The time step must be adequately small to maintain stability conditions.

When the algorithm is used to solve static (or pseudo static) problems, dynamic relaxation procedures (DR) must be performed in order to achieve rapid convergence. To obtain static solutions, one should properly select the damping coefficient \mathbf{C} , the time increment step h , and the mass matrix \mathbf{M} , to obtain efficient convergence, determining \mathbf{x} such that $\mathbf{P}(\mathbf{x}) = \mathbf{f}$. Several approaches are available for determining the optimum convergence rate from which the optimum damping parameters will be obtained. These techniques are based on numerical error analysis of calculated value and residual of the solution. One of the approaches is developed by Bardet et al. In this project, a trial and error numerical procedure is developed for fast dynamic relaxation. The procedure is based on the equilibrium principle, when the assembly system is under static state in equilibrium. Numerical tests show that the equilibrium trial and error method is more efficient for static problems such as consolidation of soil, shaft loading tests, and other pseudo static problems.

5.5.3 Contact Mechanics

Since the DEM numerical scheme discretizes the object of interest into individual particles (or blocks) that connect or contact each other through their boundaries, the

connecting or contacting forces, and other variables of the particles, must be properly defined to accurately represent physical properties of the object. These variables include the packing form of the particle assembly, particle size distribution, density of the particles, internal configuration of particle mass, and response under different load conditions. The relationship between stress and strain and continuum equivalent of the object may be derived from the study of the force-displacement behavior between the individual particles, by using the averaging method of *the representative volume element* (RVE), as described earlier. The force calculations may vary based on different engineering problems, and may include calculations of normal force, shear force, friction, moment, and torsion of each particle at contact points. Traditionally, the contacts are considered to be elastic, so that the theory of contact of elastic bodies can be invoked to furnish a description the physical phenomena. Elastic models are widely used in DEM because the forces required to crush individual particles are much larger than the forces required to make the whole particle assembly fail, and that deformations of the individual particles are much smaller than that of the whole assembly. A well known non-linear elastic model is the Hertz-Mindlin contact model. The visco-elastic and perfect plastic model are also widely accepted in DEM. Both Hertz-Mindlin and visco-elastic models are described in this section. Note that some plastic incremental models have been proposed in recent years. These models have been very successful to describe contact problems in mechanical engineering. Since these models are stress history dependent and require significant memory to store the history of each contact of the assembly, they are not widely implemented in DEM simulations.

5.5.3.1 Non-Linear Hertz-Mindlin Contact Model

The Hertz-Mindlin model begins by assuming that contacting solids are isotropic and elastic, and that the representative dimensions of the contact area are very small compared to the various radii of curvature of the undeformed bodies. Another

assumption of the Hertz-Mindlin model is that the two solids are perfectly smooth. Only the normal pressures that arise during contact are considered (the extensions of Hertz theory for the tangential component of traction will be discussed later). The Hertz-Mindlin contact-force-displacement law is nonlinear elastic, with path dependence and dissipation due to slip, and omits relative roll and torsion between the two spheres. Strictly speaking, the simplified contact force-displacement law is thermodynamically inconsistent (i.e., unphysical), since it permits energy generation at no cost. The law is widely used in engineering because of its simplicity. For the particle assembly, the contact forces and displacements are infinite, and the approximation satisfies the accuracy of engineering applications.

The normal force-displacement relationship of the Hertz-Mindlin law is:

$$N = \frac{4E_0}{3\sqrt{R_0}} \rho^{3/2} \quad (5.21)$$

where (as shown in Figure 5.4 and Figure 5.5)

N is normal force

ρ is the relative approach of the sphere (Figure 5.4)

R_0 is the average radius of two contact spheres

$$\frac{1}{R_0} = \frac{1}{R_1} + \frac{1}{R_2} \quad (5.22)$$

where

R_1 and R_2 are the radii of sphere 1 and sphere 2, respectively

E_0 is the average modulus of the materials of two contact spheres

$$\frac{1}{E_0} = \frac{1-\nu_1^2}{E_1} + \frac{1-\nu_2^2}{E_2} \quad (5.23)$$

where

E_1 and E_2 are Young's modulus

ν_1, ν_2 are Poisson's ratio of sphere 1 and 2, respectively

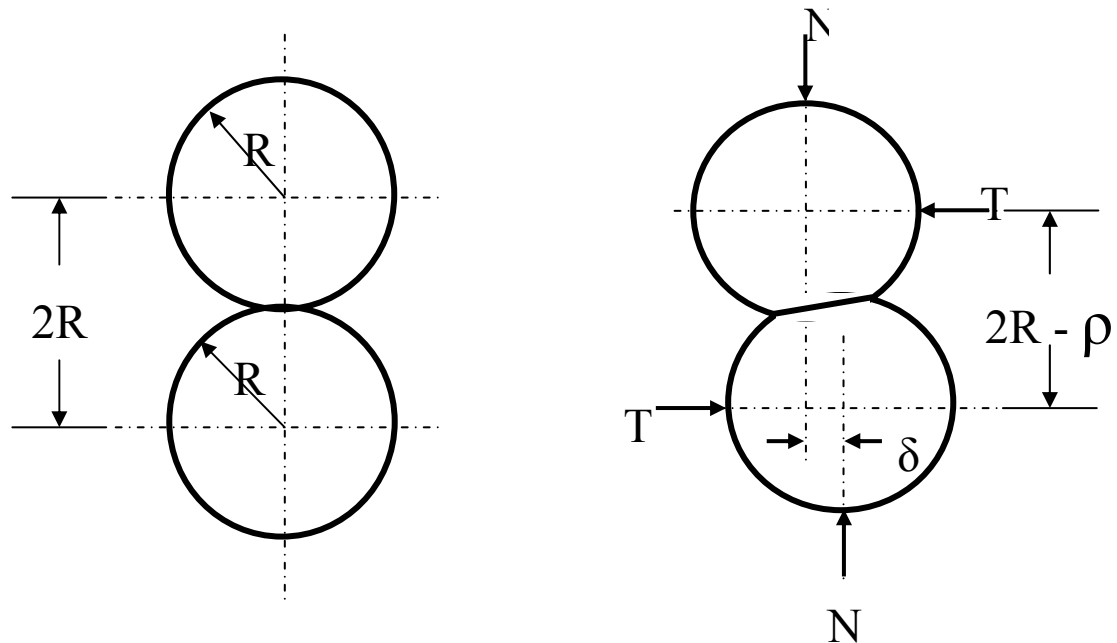


Figure 5.4 Identical Elastic Rough Spheres in Contact

Tangential force-displacement is one of the important extensions of the Hertz contact law, which addresses problems involving additional force systems superimposed upon the Hertz normal force. By solving the appropriate boundary-value problem, Cattaneo and Mindline derived expressions for the tangential component of traction on the contact surface, and the displacement of points on one sphere, remote from the contact, with respect to similarly situated points in the other sphere. Physical experiments show that slip occurs between two contact spheres no matter how small the applied tangential force. When the tangential force is completely removed, the

slip does not vanish. A permanent displacement appears. This displacement can be removed only by applying a tangential force in the opposite direction. For this reason, the tangential forces are calculated separately for different cases. Three cases in tangential force-displacement calculations are considered:

- increasing tangential force
- decreasing tangential force
- oscillating tangential force

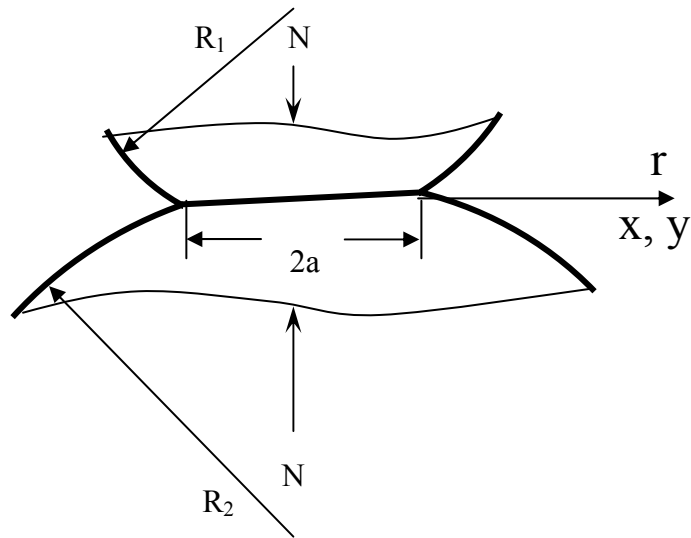


Figure 5.5 Hertz Contact of Solids of Revolution

Case 1. The tangential force-displacement relationship of increasing tangential force with consideration of slip conditions is given by:

$$\delta = \frac{3(2-\nu)fN}{8Ga} \left[1 - \left(1 - \frac{T}{fN} \right)^{2/3} \right] \quad (5.24)$$

where

δ is relative displacement proportional to the tangential applied force

ν is Poisson's ratio

G is shear modulus of the material

a is contact area of two contact spheres

N is normal force obtained from equation (5.21)

f is coefficient of static friction

T is applied tangential force in contact plane

Case 2. The tangential force-displacement relationship of decreasing tangential force with consideration of slip conditions is given by:

$$\delta_u = \frac{3(2-\nu)fN}{8Ga} \left[2 \left(1 - \frac{T_s - T}{2fN} \right)^{2/3} - \left(1 - \frac{T_s}{fN} \right)^{2/3} - 1 \right] \quad (5.25)$$

where

δ_u is relative displacement proportional to the unloading tangential applied force

T_s is the tangential force at peak value $0 < T_s < fN$

Case 3 considers oscillating tangential force-displacement relationship. A subsequent increase of T from $-T_s$ to T_s will give rise to identical events as occurring in the course of the reduction of T from T_s to $-T_s$, except for the reversal of sign. The appropriate displacement during this loading process will be $\delta_l = \delta_u(T)$.

5.5.3.2 The Visco-Elastic Contact Model

The visco-elastic contact model is the simplest contact model used in DEM simulations. Because of its simplicity, the calculations are very efficient. Usually,

the stresses causing the failure of particle assemblies due to the relative friction and slip between the particles are much lower than the stresses required to crush individual particles. The assumption of a linear elastic contact force-displacement relationship between two particles is a good approximation, and is still widely used in engineering. The mechanical model is shown in Figure 5.2.

The normal contact formulation is linear elastic with a viscous damper characterized by two parameters: normal stiffness k_n and viscosity C . The model works for both compression and tension forces based on the relative distance between the two contact points. The normal force is defined by:

$$\mathbf{N} = \begin{cases} \frac{1}{2}k_n \varepsilon \cdot \mathbf{n} + C\mathbf{v}_m & \varepsilon \geq 0 \text{ || } \varepsilon \geq -\varepsilon_{\max} \\ 0 & \varepsilon < -\varepsilon_{\max} \end{cases} \quad (5.26)$$

where

ε is the penetration distance between two contact points. For two spheres, ε equals the sum of two sphere's radii minus the distance between the two contact sphere centers.

$-\varepsilon_{\max}$ is the maximum tension distance two neighboring particles. If negative penetration is larger than this value, the connection between the two neighbors are disconnected, and tension force between these two particles is set to be zero.

\mathbf{n} is the normal unit vector at the contact point

\mathbf{v}_m is the normal relative velocity vector at the contact point

k_n is the normal contact stiffness

C is the viscosity of the material

The tangential force depends on the friction of the material and the relative tangential velocity of the two contact particles. The formula of the tangential force is defined as:

$$\mathbf{T} = \begin{cases} \text{sign}(\mathbf{v}_{rs}) \frac{1}{2} k_s \boldsymbol{\varepsilon} \cdot \mathbf{s} & \frac{1}{2} k_s \cdot \boldsymbol{\varepsilon} < f |N| \\ \text{sign}(\mathbf{v}_{rs}) f |N| \mathbf{s} & \frac{1}{2} k_s \cdot \boldsymbol{\varepsilon} \geq f |N| \end{cases} \quad (5.27)$$

where

k_s is the shear contact stiffness

f is the coefficient of static friction

\mathbf{v}_{rs} is the tangential relative velocity vector at the contact point

The direction of the tangential force is the reverse of the tangential relative velocity. The magnitude of tangential force is equal to the maximum static friction force, if it is bigger than the Coulomb friction force, which is the second term of equation (5.27).

The key to successful modeling using DEM is proper selection of the stiffness and damping coefficients. Theoretically, the damping coefficient can be derived from material properties such as the restitution coefficient:

$$C = 2 \ln\left(\frac{1}{e}\right) \sqrt{\frac{k_n m_i m_j}{(m_i + m_j) \pi^2 + [\ln(1/e)]^2}} \quad (5.28)$$

where

m_i and m_j are the masses of particles i and j , respectively.

e is the restitution coefficient of the material

k_n is the normal contact stiffness

To relate the stiffness to material properties, a number of trial and error numerical tests are performed. The procedures are based on the principle of elastic wave propagation in a medium, which are widely used to determine elastic constants of materials in laboratories. In the numerical tests, the particles are assembled in different packing forms, and elastic stress waves are generated. The wave propagation velocities are measured at different points for different stiffness. The stiffness is checked against the wave velocity obtained from material property manuals and laboratory data. The stiffness is then calibrated correspondingly and saved in a database for future modeling.

5.5.4 Validation of Numerical Models

Before the numerical model is applied to solve engineering problems, it is used to simulate some small scale problems and simple cases for which the results are known or can be easily obtained, for verification. Some constants and parameters must be pre-defined or calibrated based on material properties and specified conditions. In this project, the validity of the numerical modeling has been checked in three different ways before being used for large scale problems: 1) energy conservation; 2) dynamic relaxation and 3) elastic wave propagation.

5.5.4.1 Energy Conservation

First, an energy method was used to verify dynamic stability of the system. The energy of an individual discrete particle in the system consists of three parts: kinetic energy, potential energy, and gravitational energy. The energy is defined as:

$$e_i = \frac{1}{2} m_i v_i^2 + \frac{1}{2} I_c \omega_i^2 + \frac{1}{2} k (\varepsilon_i / 2)^2 + m_i g z_i \quad (5.29)$$

where

m_i is the mass of the discrete particle

v_i is the translational velocity

ω_i is the angular velocity

I_c is the mass moment of inertia of the discrete particle with respect to
the mass center

k is the stiffness of the normal contact (or stretch)

ε_i is the relative approach or stretch distance of two neighboring
particles

z_i is the particle altitude relative to the calculation datum

The total energy of the system is the sum of each individual particle:

$$E_{total} = \sum_{i=1}^n e_i \quad (5.30)$$

Figure 5.6 shows a stack of spherical elements used for the energy tests. The bottom element is not allowed to move. The remaining elements are stacked with no initial contact forces.



Figure 5.6 Stack Balls Setup for Energy and Dynamic Relaxation Numerical Tests

If there are no interactions which cause mechanical energy loss, such as damping, friction, etc., and no energy is added to the system, the total energy of the system should be conserved. For the energy test, the stack is assumed to be perfectly elastic. Under the only gravitational force, when the stack is released from the initial position, the elements will push into each other and continue to oscillate up and down forever, conserving total energy. For the stack, the diameters of all elements are equal to 1 m. The specific weight of the material is 3000 kg/m^3 , the mass of each ball is 1.5708 kg and the gravitational acceleration is 9.81 m/s^2 . The coordinate of the center of the bottom ball is set at $(0, 0, 0)$. The total energy of the stack at the beginning of the test is only gravitational energy, which equals 554.74 N-m . Figure 5.7 shows, as expected, the total energy of the stack is constant, with some fluctuations due to the numerical approximation.

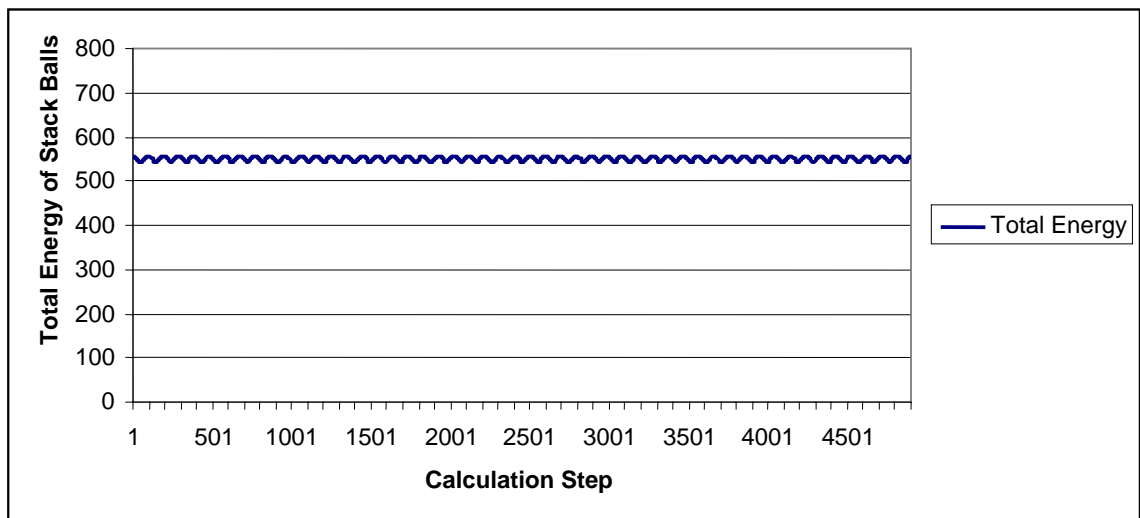


Figure 5.7 Total Energy of Stack Ball

5.5.4.2 Damping and Dynamic Relaxation (DR) Tests

Damping and dynamic relaxation (DR) are major parameters and procedures in DEM modeling for two reasons. First, the materials in this project are not elastic (i.e.

concrete and soil). Stress wave propagating in the materials are attenuated with distance. Second, since DEM is originally designed to solve dynamic problems with explicit integration for static (or pseudo static) problems, dynamic relaxation procedures (DR) must be performed in order to achieve convergence. An excessively small damping coefficient leads to spurious vibrations during the dynamic transition between two static states. This causes changes in the grain arrangement, since frictional material is very sensitive to vibrations. If the damping coefficient is too large, the results will simulate viscous flow, a phenomenon which is more related to Stokes flow of immersed bodies.

The same stack setup for the energy conservation test is used for the damping and DR tests. The diameters of the balls, specific weight, and coordinates are the same as used in the energy test. The validity of static convergence is verified by checking the displacement of the top ball on the stack under gravitation force alone. Three cases were performed for the numerical tests:

- The stack was released from the initial position without damping (restitute coefficient is zero). This test is equivalent to the elastic energy test, except that the displacement of the top is recorded.
- The same test as above with a restitution coefficient of 0.2 (damping and restitution are related by equation 5.27).
- The adaptive numerical equilibrium DR test. This algorithm is a numerical trial and error approach developed for fast convergence and stable solution. The method is based on the equilibrium principle when the assembly system is under static state at equilibrium.

As shown in Figure 5.8, the top element on the stack oscillates around its balance position when the system is released from its initial position without damping. When the normal DR procedure is performed with damping, the vibration attenuates, and

the top element position approaches a static position at 7.86 after one thousand iterations. Adaptive equilibrium DR shows that the top ball approaches the same static position faster. The adaptive equilibrium DR has a dramatic advantage in computational efficiency when the system consists of a large number of particles (i.e. thousands or millions particles).

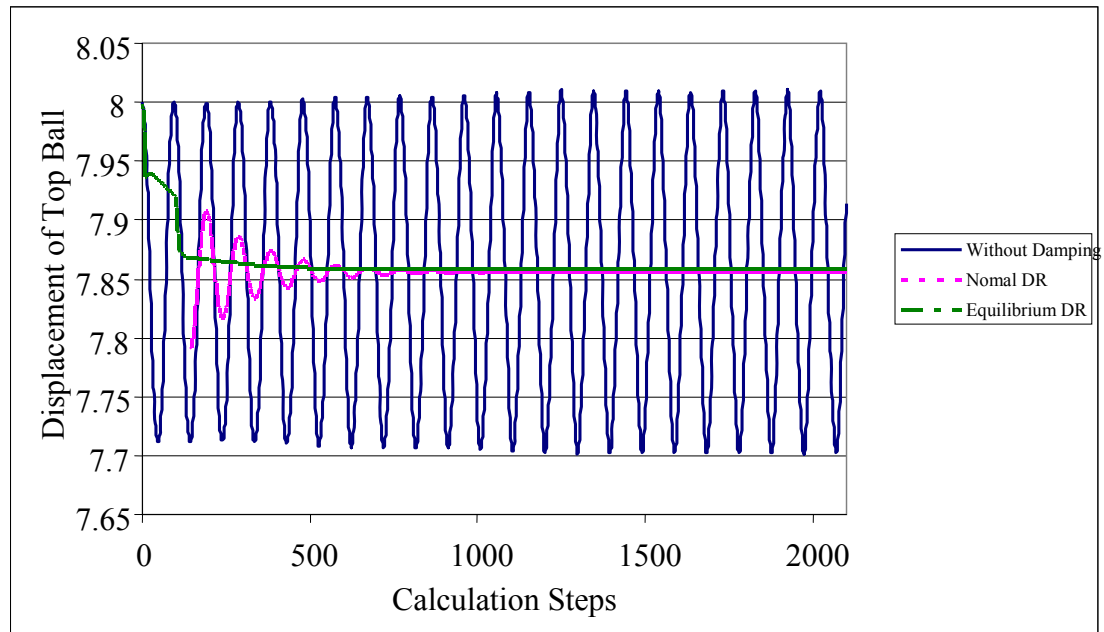


Figure 5.8 Dynamic Relaxation Test Results

5.5.4.3 Wave Propagation

To validate the wave propagation behavior of the model, the impulse response of a non-linear 1D oscillating system is obtained. The system is similar to the stack as described before, but with more elements, different material properties, and zero gravitational body forces. The system consists of one hundred identical balls with individual mass m connected with nonlinear springs of stiffness k and dashpot c . The model is simple, but useful for analyzing a wide range of dynamic systems, such as ionic polarization at the molecular level, the response of experimental devices such as

isolation tables and resonant instruments, the vibration of a foundation, and the seismic response of buildings. For 1D problems, equation (5.15) can be written as:

$$m \ddot{y}_n + c_i \dot{y}_n + k_i y_n = x_n \quad (5.30)$$

where

x is the time history of the input force. In this numerical test, x is an impulse force.

y is the time history of the displacement response. Dots on y denote first and second derivatives.

The specific weight of the material is 3000 kg/m^3 , the mass of each ball is 1.5708 kg , the gravitational acceleration is 0.0 m/s^2 , and the restitution coefficient is 0.3 (related to the damping coefficient by equation 5.28).

A vertical impulse force is applied on the top ball at its center, and the bottom ball is not allowed to move. The impulse P-wave propagates down the stack, and the wave reflects when it reaches the bottom element. The acceleration of each ball is recorded in Figure 5.9. A hundred signals are plotted as time vs. receiver distance from the source. This figure clearly shows that the first arrival delay and attenuation with distance. The first arrival is sharp, with higher frequency, for the receivers closer to the source, and flattens with distance. The plot also shows the reflection from the bottom.

The test shows that the model is able to successfully propagate waves in different materials with various boundary and initial conditions. The model provides a fundamental and powerful tool for a wide range of geotechnical and civil engineering applications, such as refraction, reflection, reverse time, tomography, and other

inverse problems. With the implementation of non-reflection boundary conditions, the model is also able to simulate wave propagation in semi-infinite or infinite media.

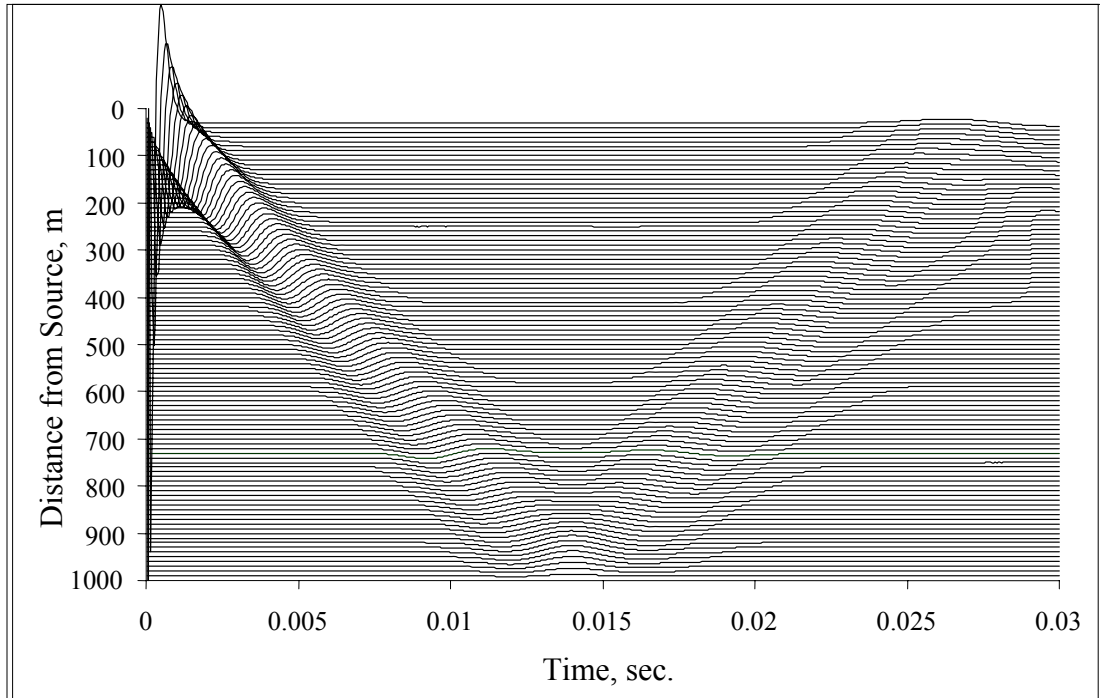


Figure 5.9 1-D P-Wave Propagation in a Rod